NUMERICAL INVESTIGATIONS ON FLOW CHARACTERISTICS OVER A CAVITY RELATING PRESSURE FIELD AND COEFFICIENT OF PRESSURE THROUGH LES-APPROACH

Dr. Nirmal Kumar Kund

Associate Professor, Department of Production Engineering
Veer Surendra Sai University of Technology, Burla 768018, India

Abstract—A proper numerical model is developed to investigate supersonic flow over a 3D open cavity. The studies on supersonic flow over the 3D cavity having length-to-depth ratio of 2, include the supersonic free-stream Mach number of 2 as well as the flow Reynolds number of 10^5. The numerical simulation has been carried out by using the Large Eddy Simulation (LES) technique. The Smagorinky model is incorporated for this investigation. The predicted results have been compared with the experimental and simulation results available in the literature. The results have been demonstrated in the form of both coefficient of pressure (Cp) and overall sound pressure level (OASPL) at the centreline of the front wall of the stated open cavity. The coefficient of pressure appears to match both qualitatively and quantitatively with the existing experimental and numerical results reported by the other investigators. Nevertheless, the overall sound pressure level at the centreline of the front wall of the said open cavity is over-predicted by approximately 40-80 dB. Furthermore, the feedback loop mechanism of the cavity has also been described. Pretty large pressure fluctuations are witnessed inside the cavity and hence these must be supressed. Nonetheless, the inclusion of a spoiler is also planned for future to alter the flow behaviours inside the cavity which may bring about the reduction in both pressure oscillations and overall sound pressure level at the centreline of the front wall of the stated open cavity.

Keywords—Numerical, Cavity, LES, Pressure Field, Coefficient of Pressure, OASPL.

I. INTRODUCTION

In our everyday life we experience aerodynamic noise from sources like exhaust pipes, vacuum cleaners, ventilation systems, fans etc. Similar is the case in many engineering applications relating to automotive sectors. It may reason for awkwardness to individuals and also disturb the furtiveness of tasks. Airframe noise is an extensive element of overall noise, mostly while landing as well as take-off. Noise from landing gear, flaps, slats etc. are considered as airframe noise. One of the greatest noteworthy airframe noises is the cavity noise. They occur from open wheel wells after the undercarriage while landing. The weapon bays in the military aircrafts also feel oscillations induced by the flow that can stimulate the vibrational modes of the entire aircraft body.

At low Mach numbers for surface transportation, the automobile company is worried with the noises produced from the door gaps, side mirrors, in addition to the open sun roof. These noises productions also influence the ease in the vehicle. The door gaps, wheel wells and weapon bays may be modelled as rectangular cavities and the poised flow outside the cavity may be considered to be constant. Despite the fact, the rectangular cavity is simple in shape, it is very rich in various dynamic as well as acoustic phenomena, likely covered by an aeroacoustic feedback loop depending on the shape/size of the cavity in addition to the flow situations. Very severe tone noises may be created as a result of the vortex shredding at the upstream edge of the cavity, while the flow past a cavity.

Heller et al. [1] illustrated on flow-induced pressure oscillations in shallow cavities. Tam and Block [2] studied on the tones and pressure oscillations induced by flow over rectangular cavities. Kaufman et al. [3] reported on Mach 0.6 to 3.0 flows over rectangular cavities. Sweby [4] applied high resolution schemes using flux limiters on hyperbolic conservation laws. Rizzetta [5] performed numerical simulation on supersonic flow over a three-dimensional cavity. Anderson and Wendt [6] described about the fundamentals of computational fluid dynamics. Piomelli [7] demonstrated on achievements and challenges of large-eddy simulation. Hamed et al. [8] conducted numerical simulations of fluidic control for transonic cavity flows. Li et al. [9] carried out LES study of feedback-loop mechanism of supersonic open cavity flows. Vijayakrishnan [10] executed a validation study on unsteady RANS computations of supersonic flow over two dimensional cavity. Sousa et al. [11] discussed about the lid-driven cavity flow of viscoelastic liquids. Tuerke et al. [12] investigated experimental study on double-cavity flow. It is understood that broad study on cavity flow has been made both experimentally and computationally for refining the aerodynamic behaviour. Nonetheless, besides its prominence, the complex flow physics associated the cavity has riveted the researchers for further investigations and remains as an interesting field of investigation.

II.   OBJECTIVES

Albeit, the flow past a cavity has been examined experimentally/numerically by many investigators, nonetheless, thorough modelling of both large and small scales of motions simultaneously, not yet done which is one of the key limitations. Conversely, Large Eddy Simulation (LES) is the technique which resolves the large eddies as it is and models the small eddies that can give realistically more reasonable results too. The motivation of this investigational work is to study the flow physics and modes of oscillations in a 3D open cavity supersonic flow. It includes particulars about the governing equations in addition to the establishment together with the application of the LES method counting the sub-grid scale modelling. The discretization techniques have also been discussed. The numerical predictions have been demonstrated in the form of pressure flow field, coefficient of pressure (Cp) and overall sound pressure level (OASPL) at the centreline of the front wall of the open cavity. The numerical results of supersonic flow over the open cavity have also been compared with the prevailing experimental/numerical results reported in the literature. In overall, very good agreement between the above-mentioned results is also witnessed from the present studies. But, the investigations relating to the usage of passive control techniques/devices for the reduction of pressure oscillations inside the cavity is planned for future. Because these devices operate over an extensive range of parameters and also very significantly influence the flow characteristics of incoming boundary layer by covering efficient flow circumstances.

III.   DESCRIPTION OF PHYSICAL PROBLEM

Supersonic flow past a three-dimensional cavity is studied numerically. The streamwise length, depth and spanwise length of the cavity are 20 mm, 10 mm, and 10 mm, respectively. The length-to-depth ratio (L/D) for the cavity is 2. The width-to-depth ratio (W/D) is 1. The cavity is three-dimensional with streamwise length-to-spanwise length ratio (L/W) > 1. In addition, the Mach number of the free-stream along with the Reynolds number based on the cavity depth are taken as 2 and 10^5, respectively, for setting the inflow conditions.

3.1. Geometric model

The computational domain of the cavity used in the present simulation is shown in figure 1. The size of the computational domain, as mentioned earlier, is 2D×D×D (length × breadth × width). The inlet boundary is located at a distance of D upstream from the leading edge of the cavity. The outlet boundary is located at a distance of 4D downstream from the trailing edge of the cavity. The upper boundary is also located at a distance of 4D above the cavity.
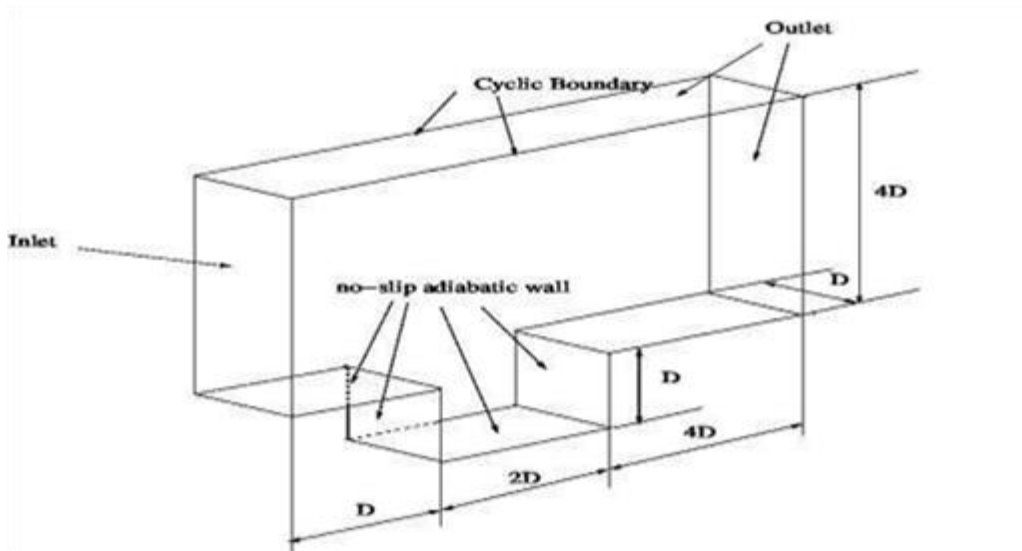
Figure 1. Computational domain of cavity

3.2. Initial and boundary conditions

The inflow boundary conditions are initialized with free-stream conditions of $M_\infty = 2$, $P_\infty = 101.325$ kPa, and $T_\infty = 300$ K. The Reynolds number of the flow used in the simulation is 10^5, which is based on the cavity depth. No-slip adiabatic wall boundary conditions is applied at the wall boundaries. Zero-gradient condition is applied at all the outflow boundaries. Periodical boundary condition is applied in the spanwise direction of the cavity.

IV. MATHEMATICAL FORMULATION

4.1. Generalized governing transport equations

The three-dimensional compressible Navier-Stokes equations are the governing equations which include the continuity equation (1), the momentum equation (2), and the energy equation (3) which are as follows:

$$\frac{\partial \rho}{\partial t} + \nabla.(\rho \boldsymbol{U}) = 0 \tag{1}$$

$$\frac{\partial (\rho \boldsymbol{U})}{\partial t} + \nabla.(\rho \boldsymbol{U}.\boldsymbol{U}) - \nabla.\nabla(\mu \boldsymbol{U}) = -\nabla p \tag{2}$$

$$\frac{\partial (\rho e)}{\partial t} + \nabla.(\rho e \boldsymbol{U}) - \nabla.\nabla(\mu e) = -p(\nabla.\boldsymbol{U}) + \mu \left[\frac{1}{2}(\nabla \boldsymbol{U} + \nabla \boldsymbol{U}^{\mathrm{T}})\right]^2 \tag{3}$$

Where,

$\boldsymbol{U}$ = velocity vector = $u\hat{\imath} + v\hat{\jmath} + w\hat{k}$

$\frac{1}{2}(\nabla \boldsymbol{U} + \nabla \boldsymbol{U}^{\mathrm{T}})$ = strain rate tensor.

The equations (1), (2) and (3) represent the conservation form of the Navier-Stokes equations. The conservation form of these governing equations are achieved from a flow model fixed in space [6]. The above equations are applicable to viscous flow, except that the mass diffusion is no included.

It is assumed, in aerodynamics, that the gas is a perfect gas. The equation of state for a perfect gas is,

$$p = \rho R T \tag{4}$$

Where, R = specific gas constant = C_p - C_v $\tag{5}$

For a calorically perfect gas (constant specific heats), the caloric equation of state is,

e = internal energy per unit mass = $C_v T$ $\tag{6}$

4.2. LES Turbulence Modelling

The turbulent flows may be simulated using three different approaches: Reynolds-Averaged Navier-Stokes equations (RANS), direct numerical simulation (DNS), and large eddy simulation (LES). Direct numerical simulation has high computational requirements. DNS resolves all the scales of motion and for this it needs a number of grid points proportional to $(Re)^{9/4}$ and computational scales' cost is proportional to $(Re)^3$ [7].

In the present study, features of the turbulent flow field have been simulated using LES as it is appropriate for unsteady complex flows as well as noise induced flows. LES computes the large resolved scales and also models the smallest scales. The turbulence model is introduced by splitting the time and space varying flow variables into two constituents, the resolved one $\bar{f}$ and f', the unresolved part:

$$(x,t) = \bar{f}(x,t) + f'(x,t) \tag{7}$$

LES uses a filtering operation to separate these resolved scales from the unresolved scales. The filtered variable is denoted by an over bar [7]. The top-hat filter smooth both the fluctuations of the large-scale and those of small scales as well. The filtering operation when applied to the Navier-Stokes equation gives:

$$\frac{\partial \bar{\rho}}{\partial t} + \nabla.(\overline{\rho \boldsymbol{U}}) = 0 \tag{8}$$

$$\frac{\partial(\overline{\rho \boldsymbol{U}})}{\partial t} + \nabla.(\overline{\rho \boldsymbol{U}.\boldsymbol{U}}) - \nabla.\nabla(\overline{\mu \boldsymbol{U}}) = -\nabla \bar{p} \tag{9}$$

$$\frac{\partial(\overline{\rho e})}{\partial t} + \nabla.(\overline{\rho \boldsymbol{U} e}) - \nabla.\nabla(\overline{\mu e}) = -\overline{p(\nabla.\boldsymbol{U})} + \mu \left[\frac{1}{2}(\nabla \bar{\boldsymbol{U}} + \nabla \bar{\boldsymbol{U}}^{\mathrm{T}}) \right]^2 \tag{10}$$

However, the dissipative scales of motion are rectified poorly by LES. In a turbulent flow, the energy from the large resolved structures are passed on to the smaller unresolved structures by an inertial and an effective inviscid mechanism. This is known as energy cascade. Hence, LES employs a sub-grid scale model to mimic the drain related to this energy cascade. Most of these models are eddy viscosity models relating the subgrid-scale stresses (τ_{ij}) and the resolved-scale rate of strain-tensor

$(\bar{S}_{ij})$,
$$\tau_{ij} - (\delta_{ij}/3) = -2\nu_T \bar{S}_{ij} \tag{11}$$

Where, $\bar{S}_{ij}$ is the resolved-scale rate of strain tensor $= (\partial \bar{u}_i/\partial x_j + \partial \bar{u}_j/\partial x_i)/2$.
In most of the cases it is assumed that all the energy received by the unresolved-scales are dissipated instantaneously. This is the equilibrium assumption, i.e., the small-scales are in equilibrium [7]. This simplifies the problem to a great extent and an algebraic model is obtained for the eddy viscosity:

$$\mu_{sgs} = \rho C \Delta^2 |\bar{S}| \bar{S}_{ij}, \ |\bar{S}| = (2\bar{S}_{ij}\bar{S}_{ij})^{1/2} \tag{12}$$

Here, Δ is the grid size and is usually taken to be the cube root of the cell volume [7]. This model is called as the Smagorinsky model and C is the Smagorinsky coefficient. In the present study, its value has been taken to be 0.2.

V. NUMERICAL PROCEDURES

5.1. Numerical scheme and solution algorithm

The three-dimensional compressible Navier-Stokes governing transport equations are discretized through a framework pertaining to finite volume method (FVM) using the SIMPLER algorithm. Here, the turbulent model used for large eddy simulation is Smagorinsky model, because of its

simplicity. The spatial derivatives such as Laplacian and convective terms are computed by second order scheme based on Gauss theorem. In addition, the viscous terms are evaluated by second order scheme. Furthermore, the implicit second order scheme is used for time integration. The numerical fluxes are evaluated by applying Sweby limiter to central differencing (CD) scheme, which is a total variation diminishing (TVD) scheme. The central differencing (CD) is an unbounded second order scheme, whereas, the total variation diminishing (TVD) is a limited linear scheme. The established solver is used to predict flow behaviours of the associated flow variables relating to supersonic flow over an open cavity.

5.2. Choice of grid size, time step and convergence criteria

Figure 2 demonstrates that the computational domain comprises of two regions: upper cavity region and inside cavity region. The grid is refined at the regions near to the wall (where very high gradient is expected) to determine the behaviour of shear layer satisfactorily. A comprehensive grid-independence test is performed to establish a suitable spatial discretization, and the levels of iteration convergence criteria to be used. As an outcome of this test, the optimum number of grid points used for the final simulation, in the upper cavity region as $360 \times 150 \times 1$ and those of in the inside cavity region as $200 \times 150 \times 1$. Thus, the total number of grid points is 84000. The values of ΔX^+, ΔY^+ and ΔZ^+ at the leading edge of the cavity are 5, 12.5 and 1.0, respectively. Corresponding time step taken in the simulation is 0.000001 seconds. Though, it is checked with smaller grids of 132000 in numbers, it is observed that a finer grid system does not alter the results significantly.

Convergence in inner iterations is declared only when the condition $\left|\frac{\varphi - \varphi_{old}}{\varphi_{max}}\right| \leq 10^{-4}$ is satisfied simultaneously for all variables, where φ stands for the field variable at a grid point at the current iteration level, φ_{old} represents the corresponding value at the previous iteration level, and φ_{max} is the maximum value of the variable at the current iteration level in the entire domain.
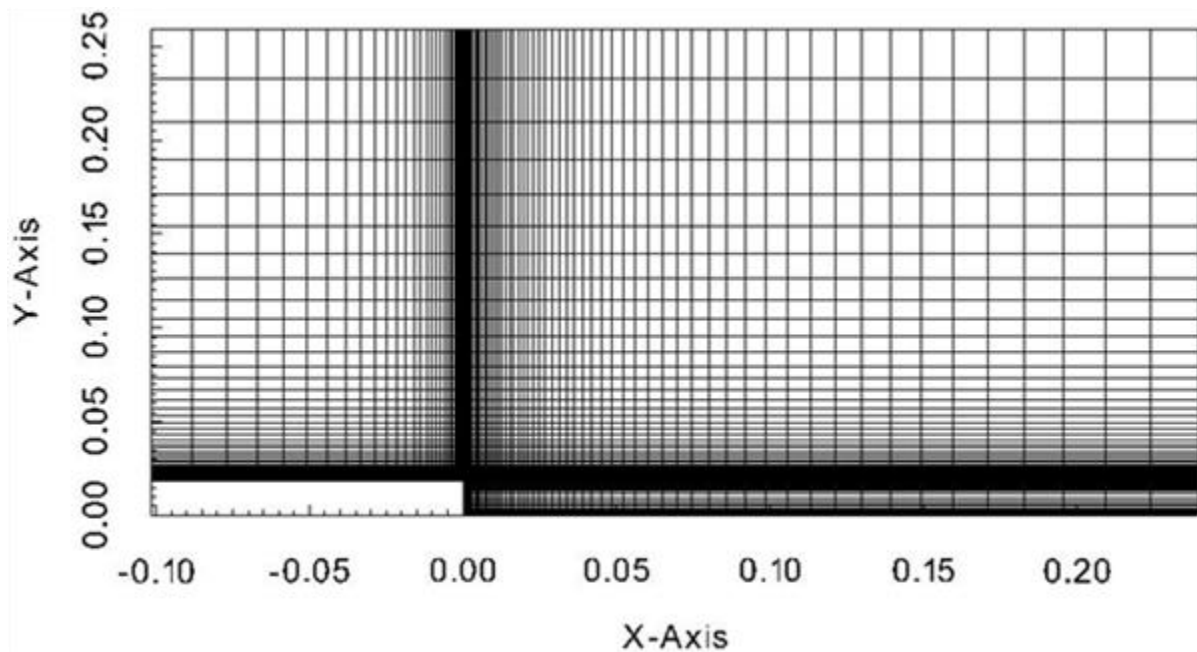

Figure 2. Computational grid of cavity in X-Y Plane

VI.   RESULTS AND DISCUSSIONS

6.1. Pressure distributions

Figures 3 and 4 illustrate the pressure fields at two different instants of times for example t = 0.1 sec as well as t = 0.3 sec, respectively. It is witnessed that a compression wave advancing forward

arrives at the front wall in addition part of the wave is reflected from the wall. This causes a backward moving reflection wave. Simultaneously, another feedback compression wave advances towards the front wall. At the centre portion of the cavity, two large vortices are observed and these vortices propagate towards the trailing edge of the cavity. Very large structured vortices strike on the aft wall and at the trailing edge a high amplitude pressure gradient is present.

The feedback compression wave arrived at the front wall, then arrives at the lip of the leading edge and thus, creates disturbance in the shear layer. The other feedback compression wave from the aft wall remains advancing towards the front wall. The front vortex, between the two vortices formed, induces inside the cavity and progrates toward the aft wall. A new compression wave is generated at the aft wall edge and travels upstream.
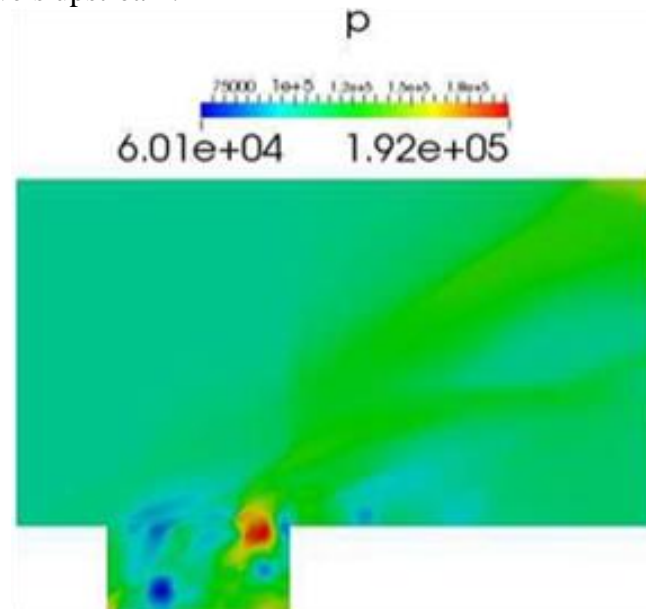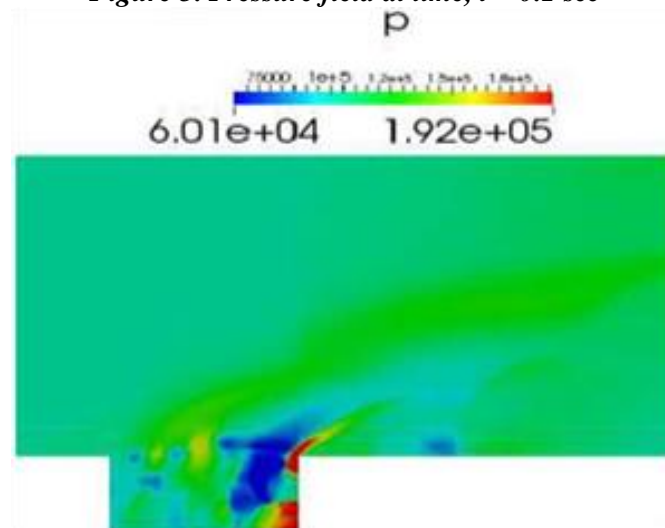

Figure 3. Pressure field at time, t = 0.1 sec

Figure 4. Pressure field at time, t = 0.3 sec

6.2. Comparisons with other numerical and experimental results
6.2.1. Comparison of coefficient of pressure (Cp)
The comparison has been done for the centreline of the front wall of the open cavity with the results of different investigators. The coefficient of pressure at the centreline of the front wall of the said cavity is demonstrated in figure 5. Furthermore, the coefficient of pressure at the centreline of the

front wall of the stated cavity is observed to be in both qualitative and quantitative agreement with the numerical simulation results reported in the literature. The variation in the results from the experimental data of Kaufman et al. is because of the numerical errors came across during the simulation practice. Additionally, the deviation from the Vijaykrishnan research work is attributable to the three-dimensionality influence and also the distinction from the Rizzetta research study is owing to the disparity in the Mach number.
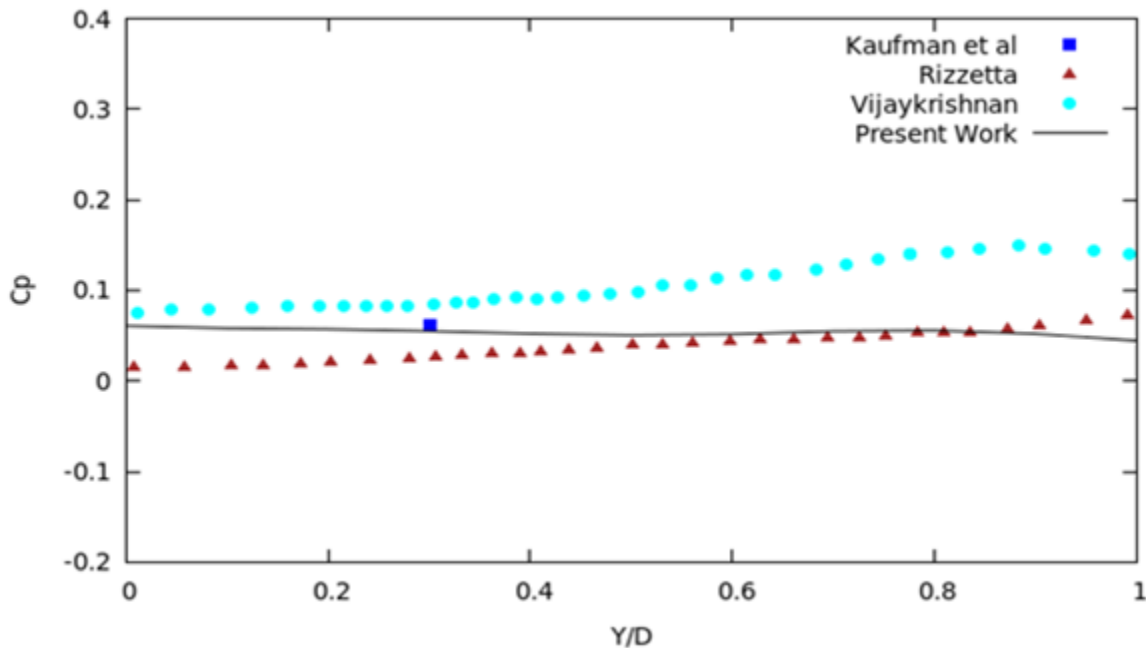

Figure 5. Coefficient of pressure at the centreline of the front wall of the cavity

6.2.2. Comparison of overall sound pressure level

The comparison has also been done with the OASPL (Overall Sound Pressure Level) distributions at the centreline of the front wall of the open cavity as obtained by different researchers. The OASPL is denoted as:

$$OASPL = 10 \, log_{10} \left(\overline{p_d^2}/q^2 \right) \tag{13}$$

Where, $\overline{p_d^2} = \frac{1}{t_f - t_i} \int_{t_i}^{t_f} (p - \bar{p})^2 \, dt \tag{14}$

q is the acoustic sound reference level with a value of 2×10^{-5} Pa
$\bar{p}$ is the time-averaged static pressure
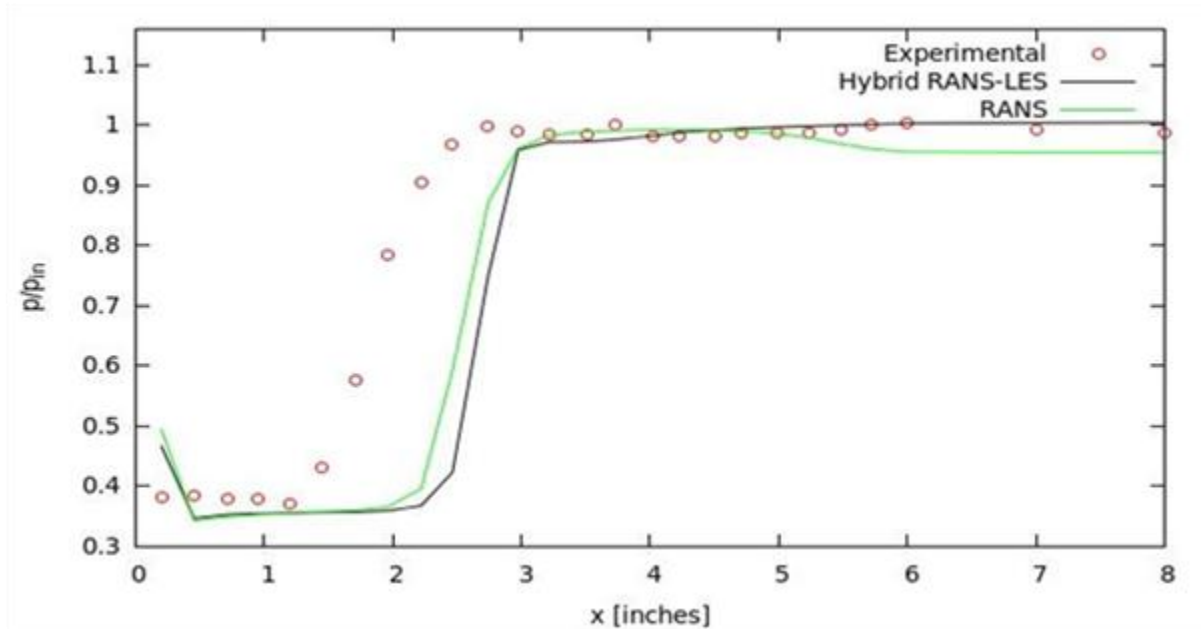t_f and t_i are the initial and final times, respectively

Figure 6. OASPL distribution at the centreline of the front wall of the cavity

The OASPL distribution at the centreline of the front wall of the stated open cavity is portrayed in figure 6. Indeed, the trend is similar to the research studies performed by the other investigators. Nevertheless, the trend is very similar to the Rizzetta research work rather than Vijaykrishnan research study. The sound pressure level attained at the front wall is nearly 5 dB higher than the aft wall. The OASPL distribution at the centreline of the front wall of the stated open cavity is over-predicted from Rizzetta research results by approximately 36-40 dB between aft and front walls. Nonetheless, the over-prediction from Vijaykrishnan research effort is almost 70-80 dB between aft and front walls. Furthermore, from the current study, the predicted sound pressure level at the centreline of the front wall of the open cavity seems to be almost uniform throughout.

VII. CONCLUSIONS

In the current study, the numerical simulations have been conducted for supersonic flow over a 3D open cavity. The cavity has length-to-depth ratio of 2 besides the Mach number of the free-stream is 2.0. The simulations are performed with LES based on Smagorinsky model for the said open cavity. The numerical simulation predictions are demonstrated in the form of both cavity flow-field (represented by pressure distribution) and aeroacoustic analyses. Additionally, the aeroacoustic analysis is also demonstrated in the form of both coefficient of pressure (Cp) and overall sound pressure level (OASPL) at the centreline of the front wall of the stated open cavity. The current numerical simulation predictions are compared with both experimental and numerical results existing in the literature. The LES model is capable to forecast all the central flow behaviours of the open cavity. Furthermore, there is both qualitative and quantitative agreement of the coefficient of pressure with the experimental and the simulation results available in the literature by the other researchers for supersonic flow over the stated open cavity. Instead, the overall sound pressure level at the centreline of the front wall of the said open cavity is over-predicted by nearly 40-80 dB. In addition, the feedback loop mechanism of the stated open cavity has also been explained. Quite large pressure fluctuations are observed inside the cavity and therefore these need to be reduced. Nonetheless, the inclusion of a spoiler in the form of one-fourth of a cylinder at the leading edge of the cavity is also planned for future to modify the flow behaviours inside the cavity that may suppress both inside pressure oscillations and overall sound pressure level at the centreline of the front wall of the stated open cavity.

ACKNOWLEDGMENTS

REFERENCES

I. Heller, H. H., Holmes, D. G., & Covert, E. E. (1971). Flow-induced pressure oscillations in shallow cavities. Journal of sound and Vibration, 18(4), 545-553.

II. Tam, C. K., & Block, P. J. (1978). On the tones and pressure oscillations induced by flow over rectangular cavities. Journal of Fluid Mechanics, 89(02), 373-399.

III. Kaufman, I. I., Louis, G., Maciulaitis, A., & Clark, R. L. (1983). Mach 0.6 to 3.0 flows over rectangular cavities (No. AFWAL-TR-82-3112). Air force wright aeronautical labs wright-patterson AFB, OH.

IV. Sweby, P. K. (1984). High resolution schemes using flux limiters for hyperbolic conservation laws. SIAM journal on numerical analysis, 21(5), 995-1011.

V. Rizzetta, D. P. (1988). Numerical simulation of supersonic flow over a three-dimensional cavity. AIAA journal, 26(7), 799-807.

VI. Anderson, J. D., & Wendt, J. F. (1995). Computational fluid dynamics (Vol. 206). New York: McGraw-Hill.

VII. Piomelli, U. (1999). Large-eddy simulation: achievements and challenges. Progress in Aerospace Sciences, 35(4), 335-362.

VIII. Hamed, A., Das, K., & Basu, D. (2004). Numerical simulations of fluidic control for transonic cavity flows. AIAA Paper, 429, 2004.

IX. Li, W., Nonomura, T., Oyama, A., & Fujii, K. (2010). LES Study of Feedback-loop Mechanism of Supersonic Open Cavity Flows. AIAA paper, 5112, 2010.

X. Vijayakrishnan, K. (2014) Unsteady RANS computations of supersonic flow over two dimensional cavity using OpenFOAM-A validation study. AIAA 2014.

XI. Sousa, R. G., et al. (2016). Lid-driven cavity flow of viscoelastic liquids. Journal of Non-Newtonian Fluid Mechanics, 234, 129-138, 2016.

XII. Tuerke, F., Pastur, L. R., Sciamarella, D., Lusseyran, F., & Artana, G. (2017). Experimental study of double-cavity flow. Experiments in Fluids, 76, 2017.